

Empirical Models for Predicting Two-Stage Light Gas Gun Muzzle Velocity

Max Murtaugh^a, Jacob A. Rogers^a, Douglas Allaire^a, Thomas E. Lacy, Jr.^{a,*}

^a*J. Mike Walker '66 Department of Mechanical Engineering, Texas A&M University, College Station, Texas, 77843.*

Abstract

Two-stage light gas guns (2SLGGs) can reliably accelerate projectiles to velocities between 1.5-8.0+ km/s and are used in hypervelocity impact, aerospace, and hypersonic research. 2SLGG operation involves a variety of physical phenomena including combustion, gas-compression, heat-transfer, and friction. Due to the wide range of operational parameters and experimental uncertainty, accurate muzzle velocity predictions can be a serious challenge. In this paper, a series of regression models for predicting muzzle velocity were fitted to and validated against 171 2SLGG launches (projectile velocities, 1.5-6.8 km/s) performed at the Texas A&M University Hypervelocity Impact Laboratory (TAMU HVIL). Most of the regression models analyzed had minimal accuracy improvement compared to basic linear regression. However, a neural network model (RMSE = 0.234 km/s) utilizing several methods to combat over-fitting, showed consistent improvement over linear regression (RMSE = 0.260 km/s) and Gaussian process regression (RMSE = 0.240 km/s). Regression model projectile velocity estimates were compared to results from the classical Piston Compression Light Gas Gun Performance (PCLGGP) and state-of-the-art LGGUN 2SLGG performance prediction codes. All of the regression models demonstrated significantly better predictive capabilities than the PCLGGP model (RMSE = 0.597 km/s), particularly at lower velocities. The regression model absolute errors from the 2SLGG experiments also compared very favorably to general absolute error estimates obtained using LGGUN. These results suggest that easy-to-implement, maintain, and scalable regression models may provide a viable alternative to complex physics-based computational models for 2SLGG launch velocity predictions, particularly as the volume of available experimental data increases. Such regression models have the potential to markedly improve predictive capabilities, identify complex coupling between experimental parameters, and reduce uncertainty.

Keywords: two-stage light gas gun (2SLGG), aeroballistic range, hypervelocity impact, regression, neural network, empirical model

1. Introduction and Motivation

1 Hypersonic vehicles and spacecraft are subjected to extreme operating environments that can adversely
2 affect mission performance. For hypersonic vehicles travelling well above the speed of sound, impacts with

*Corresponding author

Email address: TELacyJr@tamu.edu (Thomas E. Lacy, Jr.)

3 small, slow-moving atmospheric particles (rain, ice, dust, *etc.*) can be devastating. In space, micrometeoroid
4 orbital debris (MMOD) can impact spacecraft and planetary structures with relative velocities ranging from
5 2–70 km/s [1], leading to catastrophic system failure or possible loss of life. Although the impact physics
6 between the projectile and target are well-known at lower velocities, such knowledge does not directly transfer
7 to impacts at velocities exceeding roughly 2.5–3.0 km/s since the material response generally transitions from
8 strength-dominated (high-velocity) to shock/pressure-dominated (hypervelocity)¹ behavior [2]. Since the end
9 of WWII, numerous laboratories have been established worldwide to conduct hypervelocity impact (HVI)
10 research aimed at characterizing and mitigating HVIs. Many of these facilities employ a two-stage light gas
11 gun (2SLGG) to accelerate projectiles to hypervelocities. An extensive review of such 2SLGG facilities, their
12 capabilities, and research areas is presented in Rogers *et al.* [3].

13 In general, 2SLGGs can be used to efficiently accelerate projectiles to velocities between 1.5-8.0 km/s.
14 Accurate and reliable prediction of 2SLGG muzzle velocities as a function of launch parameters can be
15 extremely challenging but is essential for the execution of tightly controlled launches. Without reasonably
16 accurate predictions of muzzle velocity, multiple launches may be necessary to achieve a desired projectile
17 velocity. Moreover, replicate experiments performed at a specific velocity (with an acceptable tolerance) can
18 be difficult to perform. This can dramatically increase experimental costs and turnaround times, as well as
19 limit the utility of single experiments where repeated shots are not feasible (*e.g.*, there are a limited number
20 of targets). Thus, incorporating robust and adaptable tools for predicting launch velocities is critical for the
21 execution of a viable test plan. The actual 2SLGG muzzle velocity depends on the complex coupling between
22 a multitude of operational parameters, including gunpowder type, gunpowder mass, piston mass, burst disk
23 rupture pressure, light gas initial pressure, projectile package mass, pump tube geometry, launch tube
24 geometry, frictional forces between components, *etc.* For example, the free volume of the powder chamber
25 can profoundly affect the powder burn efficiency, compression piston acceleration profile, and energy transfer
26 to the projectile.

27 Several methods have been developed to predict 2SLGG performance and muzzle velocity. Charters *et*
28 *al.* [4] at the NASA Ames Research Center developed one of the earliest and simplest models, implemented in
29 the Piston Compression Light Gas Gun Performance (PCLGGP) software package (*i.e.*, “Charters’ code”).
30 Charters’ code has been widely adopted and is relatively easy to implement since it involves the simultaneous
31 solution of a set of linear algebraic equations. The PCLGGP model, however, makes a number of simplifying
32 assumptions that can limit accuracy (such as negligible friction, negligible heat loss, and no gas flow in the
33 pump tube). In contrast, the Simple Isentropic Compression model [5] makes fewer assumptions (accounting
34 for friction and simplified gas flow in the pump tube, as well as subsonic-to-sonic gas flow in the nozzle) but
35 is slightly more challenging to implement than the PCLGGP model since it requires the numerical solution
36 of a coupled set of nonlinear differential equations. The Richter-Von Neuman “*q*-method” [6] can account

¹For simplicity, the transition from high-velocity to hypervelocity is loosely considered to occur over the range 2.5-3.0 km/s [2].

37 for supersonic flow and shock waves in the pump tube, resulting in improvements in the predicted launch
38 velocities. The recently updated LGGUN program developed by Bogdonaff *et al.* [7, 8] at NASA Ames
39 is arguably the most sophisticated 2SLGG prediction code. LGGUN is a quasi-one-dimensional Gudonov
40 code that is second-order accurate in time and third-order accurate in space. Validation studies using
41 LGGUN report high accuracy, but the code implementation and interpretation of results requires considerable
42 expertise on the part of the user.

43 The limitations and difficulties associated with numerical 2SLGG performance prediction tools have
44 motivated the development and implementation of a few empirical approaches. Fraunhofer EMI developed
45 a neural network model to predict 2SLGG muzzle velocities in an effort to improve gun performance [9,
46 10]. However, limited information was provided regarding the neural network model’s design and accuracy.
47 Shojaei *et al.* [11] evaluated a series of regression methods for predicting 2SLGG muzzle velocities, with a
48 focus on random forest regression [12]. In the current study, we dramatically extend the work of Shojaei *et*
49 *al.* [11] by considering a more robust set of regression models. Random forest regression was not included
50 since an initial screening of regression models suggested that it did not perform as well as basic linear
51 regression. Apart from Shojaei *et al.* [11] and the current study, most techniques for predicting 2SLGG
52 performance are physics-based numerical models with, at most, empirically derived parameters. To the best
53 of the authors’ knowledge, there are no other purely empirical 2SLGG prediction studies reported in the
54 literature.

55 Since the advent of 2SLGGs (*circa* 1950) [13, 14], many computational resources and advanced regression
56 techniques have been developed which can be used to predict launcher performance. For instance, artificial
57 neural network regression [15], support vector regression [16], and Gaussian process regression with particular
58 kernels [17] are often used for nonlinear regression since they serve as “universal approximators” [18, 19] able
59 to approximate any deterministic relationship between inputs and outputs. The different regression methods
60 vary widely in their implementation, accuracy, and unique strengths.

61 In this study, a series of regression methods (linear, LASSO, ridge, elastic-net, neural network, Gaussian
62 process, and support vector) are used to predict 2SLGG performance. Specification of each regression method
63 is first presented followed by a discussion of regression results. Concluding remarks are provided and future
64 improvements to the approach are suggested.

65 **2. Methodology: HVI Experiments and Regression Models for Predicting 2SLGG Muzzle** 66 **Velocity**

67 All regression models were developed using performance data from the powder-driven 12.7 mm bore
68 2SLGG used in the Texas A&M University Hypervelocity Impact Lab (TAMU HVIL) [2]. A brief overview
69 of the 2SLGG operation and the regression models are included in the following discussion.

70 2.1. 2SLGG Operation and Experiments

71 In essence, a 2SLGG harnesses the energy generated by a single-stage launch system to compress a
72 light working gas, which ultimately drives a projectile. Typically, 2SLGGs are comprised of seven primary
73 structural and consumable elements: (1) a pressure breech, (2) pump tube, (3) central breech, (4) launch
74 tube, (5) deformable compression piston, (6) burst disk (a.k.a. petal valve), and (7) projectile or projectile
75 package (projectile + sabot). The pressure breech, pump tube, central breech, and launch tube are coaxially
76 arranged and connected with rigid coupling mechanisms and interfacing O-rings to ensure gas-tight seals [3].
77 Initially, the piston occupies the uprange end of the pump tube, and the projectile is situated at the uprange
78 end of the launch tube, just downrange of the burst disk (Figure 1a). A predetermined quantity of a low-
79 molecular-weight light working gas (*e.g.*, hydrogen or helium) is injected into the pump tube. As an aside,
80 gunpowder combustion generates the piston driver gas in most guns (~80%), but a few guns use cold-gas (He,
81 N₂, *etc.*) stored in high-pressure reservoirs, released through a fast-acting valve [3]. While cold-gas-driven
82 2SLGGs are not considered in this study, their inclusion in the future would be relatively straightforward.
83 For the HVIL gun and most other powder-driven 2SLGGs, the main (secondary) powder charge is ignited in
84 the pressure breech by a smaller, faster-burning primary charge. High-pressure combustion gases generated
85 in the powder/pressure breech are used to drive a deformable (*e.g.* polyethylene) piston downrange within
86 the pump tube (Figure 1b); this compression process rapidly elevates the pressure and temperature of the
87 working gas. When a specific burst pressure is exceeded, the burst disk ruptures, exposing the projectile to
88 the compressed working gas, which propels it down the launch tube (Figure 1c). Eventually, the projectile
89 exits the muzzle at velocities up to ~8 km/s (Figure 1d) [3]. Most 2SLGGs are accompanied by coaxial
90 range tankage that collectively form an aeroballistic range. Tankage assemblies usually include one or more
91 enclosed cylindrical tanks that contain the projectile during its free flight and/or impact. Range tankage
92 configurations and applications are largely outside the scope of this work but are summarized in Rogers *et*
93 *al.* [3]. For reference, key design parameters and capabilities of the HVIL 2SLGG are given in Table 1.

94 After the projectile package leaves the muzzle, the sabot generally must be stripped from the projectile
95 by some means. For smooth bore guns, such as that in the HVIL, sabots are separated from the projectile
96 *via* aerodynamic forces within one or more of the range tanks [3, 20, 21]. The tankage internal pressure
97 can be varied to induce different degrees of sabot separation. Of course, this separation process can also
98 decelerate the projectile. Hence, the range tankage “backfill” pressure, in addition to primary and secondary
99 powder types/masses, piston mass, piston release pressure, working gas type and initial pressure, burst disk
100 rupture pressure, and projectile package mass can be readily varied to tune 2SLGG launch conditions and
101 performance. Accurately predicting the muzzle velocity given some or all of these variables is the primary
102 goal of this work. The fundamental operation of most unaltered 2SLGGs is very similar [3], allowing this
103 study’s findings, interpretations, and predictive methods to be easily adapted to other gun configurations.

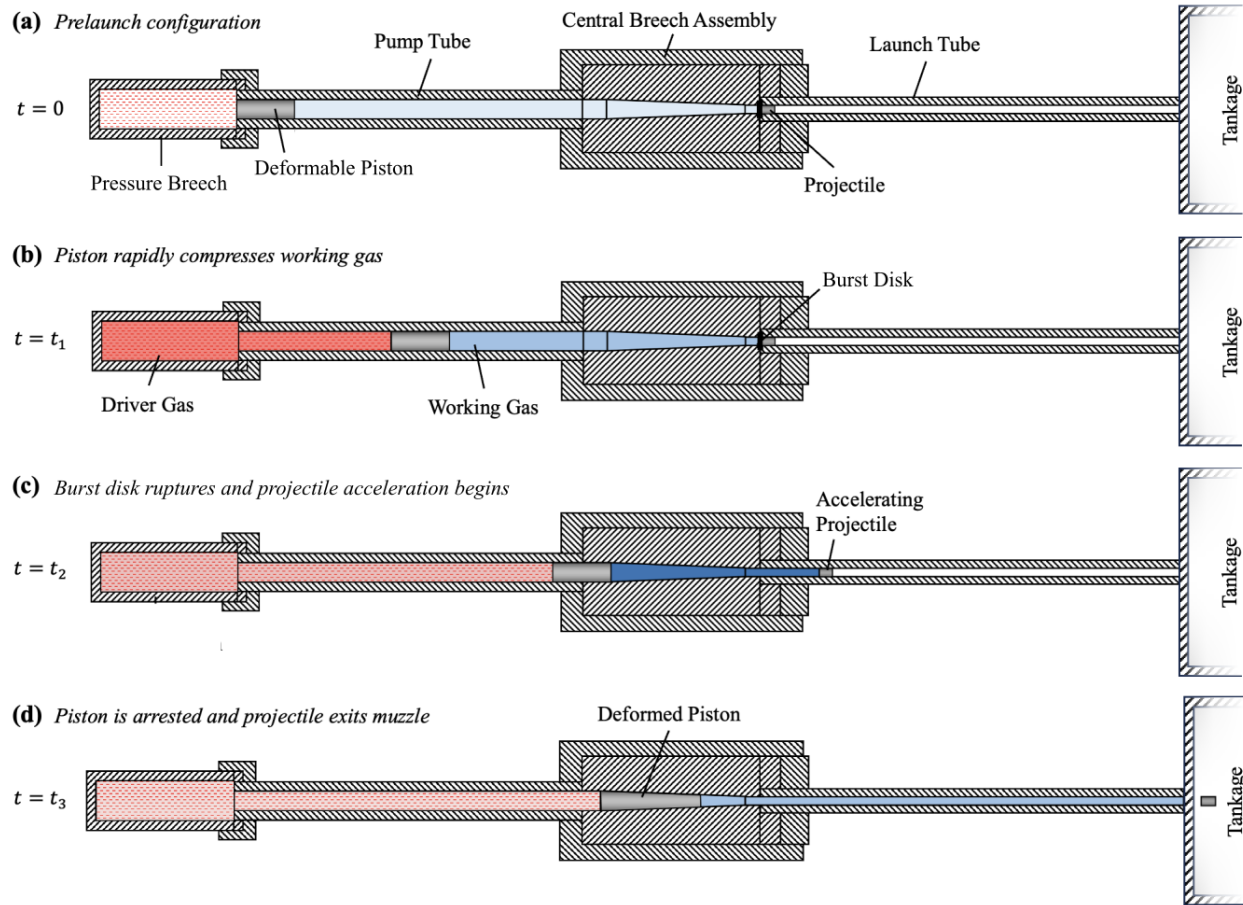


Figure 1: An illustrative guide to the operating principle of a 2SLGG, detailing (a) the moment prior to projectile launch, (b) the phase of working gas compression, (c) the instant the burst disk ruptures and acceleration of the projectile commences, and (d) immediately following the projectile's exit from the muzzle as it enters the aeroballistic range tankage. Figure reprinted with modification from Rogers *et al.* [3].

104 2.2. Variable/Feature Selection

105 In total, ten different variables (features) were used for predicting 2SLGG muzzle velocity. Most of the
 106 variables were continuous: projectile package mass, primary powder mass, secondary powder mass, pump-
 107 tube fill (working gas) pressure, and tankage (backfill) pressure. The steel burst disk rupture pressure was
 108 varied by changing the disk's score depth. This score depth was treated as quasi-discrete since only two depths
 109 were considered. The primary powder type and mass were not the only variables that influenced the pressure
 110 profile in the powder breech (and thus piston acceleration in the pump tube): changing the internal volume
 111 of the powder breech for a given powder mass resulted in more efficient powder combustion. Increasing the
 112 piston release pressure had a similar effect. The powder breech internal volume was varied by incorporating
 113 volume reducers. The number of volume reducers was treated as a discrete variable. Changes in piston
 114 release pressure were somewhat controlled by discrete variations in the piston frictional fit within the pump
 115 tube. The piston release pressure was treated as a *subjective* discrete variable characterized in terms of how
 116 "tightly" the piston fit into the uprange end of the pump tube; "low," "med," or "high" levels of tightness

117 corresponded with parameter values of 0.0, 0.5, and 1.0, respectively. Finally, five categorical features were
 118 used to represent the five different gun powders employed in previous experiments: H4831 [22], H4831SC [22],
 119 IMR 4831 [23], 50BMG [22], and SW50BMG [24]. The 50BMG and SW50BMG powder burn data needed for
 120 PCLGGP predictions were not available at the time of this publication. Hence, to compare with PCLGGP
 121 predictions, data using these powders was omitted. However, the full-scale laboratory implementation of the
 122 regression model for 2SLGG muzzle velocity is trained on more of the data which includes all powder types.

123 2.3. Model Validation and Hyperparameter Tuning

124 A regression model is only useful so far as it can accurately predict new data. Since models can overfit
 125 data (accurately predicting given data but mispredicting new data) the only reliable metric for a regression
 126 model’s performance (*i.e.*, accuracy) is how well it predicts “unseen” data that was not used to fit the model.
 127 In practice this means that some of the data must be withheld during the training process to validate model
 128 performance afterwards. A common method is holdout validation which involves partitioning the data into
 129 a training set (for fitting the model) and a testing set (for validating model performance) [25]. Determining
 130 how much data to withhold for testing presents a nuanced challenge, particularly for smaller datasets. The
 131 training set needs enough data to construct a robust model while the testing set needs enough data to give
 132 a reliable and representative estimate of model performance. [25]

133 During training, parameters (analogous to model coefficients) are fit to match the training data through
 134 some sort of optimization process (*e.g.*, gradient descent [26]). However, some regression models contain both
 135 parameters (optimized during the training process) and hyperparameters which affect the training process
 136 and must be decided beforehand. Examples of hyperparameters include the learning rate, number of training
 137 iterations, penalty terms, and the number of layers in a neural network. These hyperparameters can have a
 138 significant impact on a model’s performance but must be determined outside of the model’s typical training

Table 1: Key design and operational parameters for the TAMU HVIL 2SLGG [2]. Regression model parameters are indicated with an asterisk (*).

| Parameter | Value |
|--|--|
| 2SLGG total length (m) | 13.70 |
| Pump tube inner diameter (mm) | 44.00 |
| Pump tube length (m) | 3.70 |
| Launch tube inner diameter (mm) | 12.70 |
| Launch tube length (m) | 3.70 |
| Single-projectile diameter range (mm) | 2.0–12.7 |
| Achievable projectile velocity range (km/s) | 1.5–8.0 |
| Maximum rated kinetic energy (kJ) | 80.00 |
| Projectile package mass* (g) | 2.0–6.1 |
| Primary powder mass* (g) | 1.0–2.0 |
| Secondary powder mass* (g) | 50–165 |
| Pump tube fill (working gas) pressure* (MPa) | 0.96–1.93 |
| Tankage (backfill) pressure* (kPa) | 0.0–66.0 |
| Piston Mass* (g) | 350–800 |
| Burst disk score depth* (mm) | 0.36, 0.51 |
| Piston Fit Tightness* | low (0.0), medium (0.5), high (1.0) |
| Powder chamber volume* (cm ³) | 172.6, 265.5, 424.8 |
| Secondary powder type* | H4831, H4831SC, IMR 4831, 50BMG, and SW50BMG |

139 process. To create better models, hyperparameters are often tuned algorithmically to achieve the best model
 140 performance on some unseen data set (tuning data). Like the testing set, the tuning set gives an estimate of
 141 how well the model predicts unseen data with specific hyperparameters. However, the tuning set and testing
 142 set must be disjoint to avoid “peeking:” including testing data in the hyperparameter tuning process. Once
 143 the testing data has been *peeked* it is no longer truly unseen data which risks overfitting and can bias the final
 144 results. A simple method for segmenting the testing, tuning, and training sets is to first partition the data
 145 into a training and testing set and then further partition the training set into a tuning set and final training
 146 set as demonstrated in Figure 2. Since hyperparameter tuning shrinks the training set, it makes training
 147 robust models on limited data more difficult. For this reason, using the final hyperparameters, the model is
 148 typically retrained on the combined training and tuning data before validating the model’s performance on
 149 the testing data.

150 To alleviate the problems with holdout validation on small data sets, cross-validation can be used in-
 151 stead [25]. In k -fold cross-validation, the data is partitioned into k subsets (usually 5-10). For each subset,
 152 a model is trained on the other $k - 1$ subsets combined and tested on the original subset. If this is done for
 153 each subset, the aggregate results give a measure of model performance based on all data while still using
 154 $(k - 1)/k$ of the data to train each model. This gives a more reliable and representative measure of model
 155 performance while still using sufficient data to train robust models. A drawback of cross-validation is its
 156 computational cost, as it requires the model to be trained k times instead of just once. However, when
 157 several models are trained on slightly different data (as in each fold), the predictions can be averaged to give
 158 a result less prone to overfitting. This is referred to as k -fold averaging [27] and is one of many ensemble

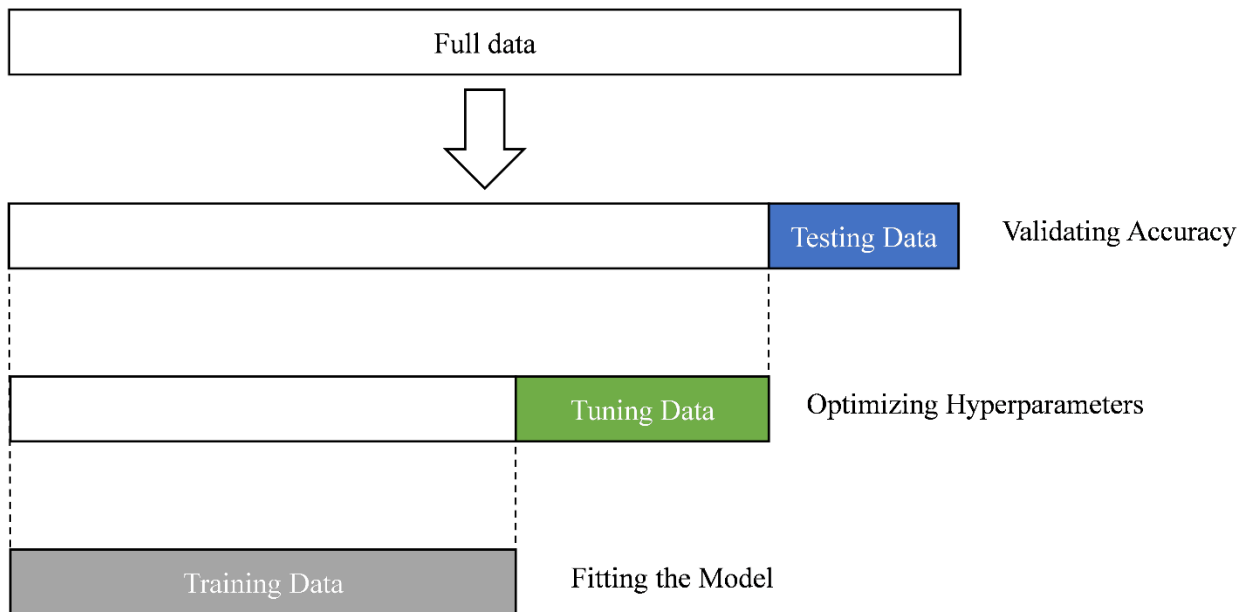


Figure 2: Illustration of data partitioning for hyperparameter tuning and model validation using basic holdout validation.

159 methods [28] used to combat overfitting in regression models.

160 Adding hyperparameter tuning to k -fold cross-validation can be accomplished in two different ways. The
161 simplest option is to partition the training set into a single training and tuning set for each fold like in
162 holdout validation. Another option is to split the training set into several subsets to perform *nested* cross-
163 validation [29] which uses all the *training* data to optimize hyperparameters in the same way non-nested cross
164 validation uses all the data to validate model performance. The recursive data partitioning involved in nested
165 cross-validation is demonstrated in Figure 3 where an outer loop (a) is used to validate model performance and
166 within each of these outer loops another inner loop (b) is used to optimize the hyperparameters. Nested cross-
167 validation often leads to higher computational costs without added benefit [29], but was deemed necessary
168 in this study to utilize k -fold averaging.

169 In this study, the regression model performance varied dramatically depending on which data points were
170 used in the test set (some being easier or harder to predict than others) due to the limited number of data
171 points (171, see Appendix A) and large number of variables (10). As such, five-fold cross-validation was used
172 to give a more reliable estimate of model performance. For regression models needing hyperparameter tuning,

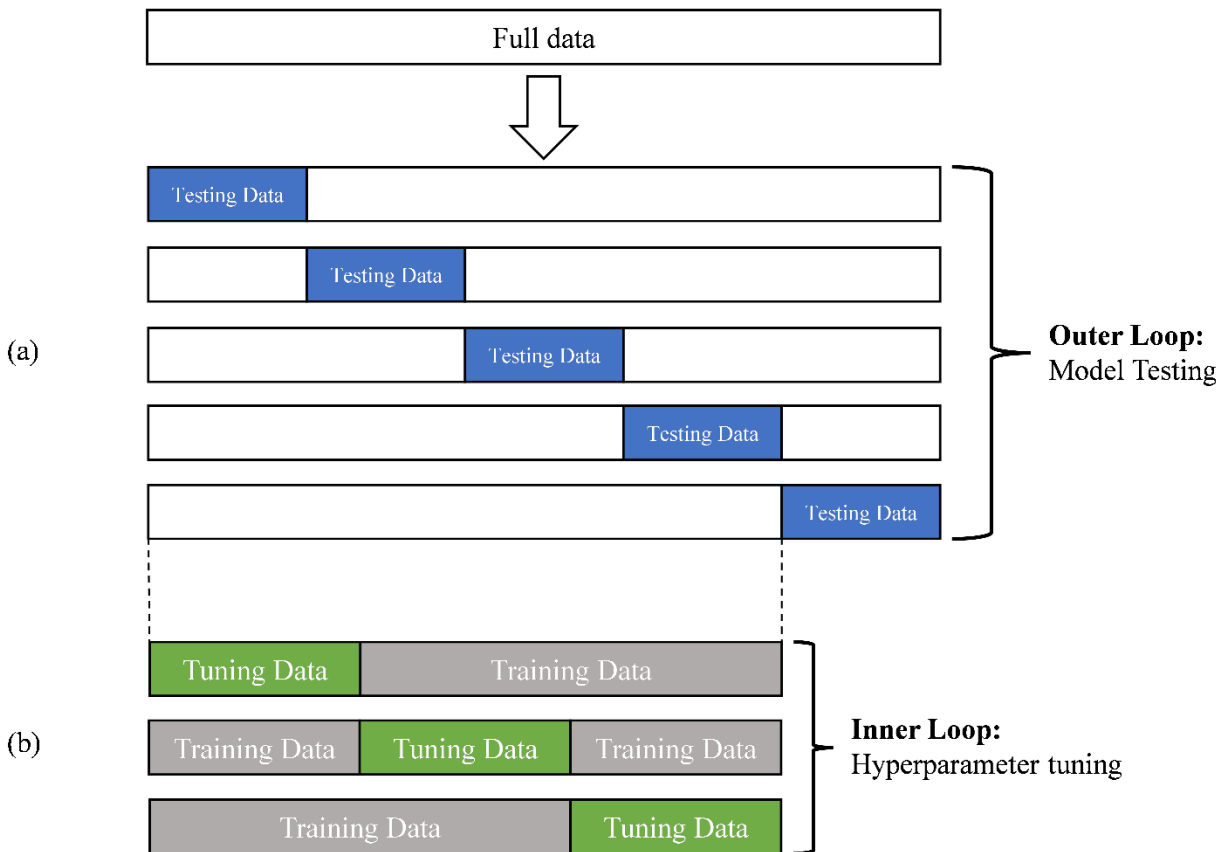


Figure 3: Pictorial demonstration of recursive data partitioning in nested cross-validation with five-fold cross-validation in the outer loop (a) and three-fold cross-validation in the inner loop (b).

173 hyperparameters were optimized using the Tree-Structured Parzen Estimator method [30] and nested cross-
 174 validation (five outer and inner folds) was employed to leverage k -fold averaging. This approach minimized
 175 overfitting by averaging predictions from all models in the inner loop, rather than retraining a single model
 176 with the combined training and tuning data.

177 2.4. Regression Methods

178 The most basic form of regression is linear least-squares regression, which determines the weights (co-
 179 efficients) that minimize the squared residual error. LASSO [31], ridge [32], and elastic-net [33] regression
 180 function nearly identically to linear regression but add a penalty term (abbreviated as P) to the squared
 181 error that is related to the magnitude of the weights $\{w_i\}$:

$$\text{LASSO: } P = \lambda_L \sum |w_i|, \tag{1}$$

$$\text{ridge: } P = \lambda_R \sum w_i^2, \tag{2}$$

$$\text{elastic-net : } P = \lambda_L \sum |w_i| + \lambda_R \sum w_i^2, \tag{3}$$

182 where λ_L and λ_R are hyperparameters for scaling the penalty term. This encourages the regression model to
 183 assign zero weights to variables that only marginally improve results which reduces over-fitting. A penalty
 184 term of zero ($\lambda_L = \lambda_R = 0$) makes all three methods identical to basic linear regression.

185 These linear regression methods can be expanded to higher order polynomial regression (*e.g.*, quadratic)
 186 by using a higher order expansion of the independent variables. For example, a linear model with independent
 187 variables x_1 , x_2 and dependent variable y can instead be expressed using a quadratic form:

$$z_1 = x_1, \quad z_2 = x_2, \quad z_3 = x_1x_2, \quad z_4 = (x_1)^2, \quad z_5 = (x_2)^2. \tag{4}$$

188 Then the relationship $f(z_1, z_2, z_3, z_4, z_5) = y$ can be fit using linear regression (just with more variables)
 189 and is equivalent to a quadratic regression of the relationship $g(x_1, x_2) = y$. This is less useful for more so-
 190 phisticated regression methods which can intrinsically derive higher order relationships (*e.g.*, neural network
 191 regression) but is essential for modeling more complex phenomena with linear regression methods.

192 Support vector regression [16] is more complicated than the LASSO, ridge, and elastic-net methods and
 193 seeks to find a curve that represents the data with maximal error (ϵ) between the curve and experimental
 194 values. Anything within $\pm\epsilon$ is treated the same whether the error is 0 or 0.99ϵ . This helps create a curve that
 195 fits the data within acceptable margins while avoiding over-fitting. Since ϵ is a user-specified hyperparameter,
 196 the problem can often be over-constrained at which point some “slack” beyond ϵ is allowed but minimized.

197 Gaussian process regression [17] is based on Bayesian statistics where prior “beliefs” (assumptions on

198 probability) are updated based on new information. Gaussian process regression starts by assuming some
199 prior distribution of functions and then updates this distribution based on given data. Instead of assuming
200 a specific function for predicted model output, Gaussian process regression gives a distribution of functions
201 with common properties (*e.g.*, differentiability, periodicity, and how close two points need to be to affect
202 each other). In a simple case with no experimental error, giving the algorithm several data points updates
203 the prior distribution of functions to a new (posterior) distribution where all functions pass through the
204 given data points. From this new distribution, the expected value (or mean) at a specified point is the
205 prediction of the model. Noisy inputs can be easily accounted for by adding a hyperparameter for the
206 variance (or experimental error/noise) of the training data (σ_n^2) to the model. Unlike other regression
207 methods, Gaussian process regression can give an estimate of the variance (*i.e.*, uncertainty) of a prediction
208 using the variance of the posterior distribution at the specified point. However, Gaussian process regression
209 can become computationally expensive on larger data sets due to the inversion of an $N \times N$ matrix, where
210 N is the number of data points. In addition, difficulties may arise from an excessive number of features
211 such as in image recognition. For this study, the Gaussian process regression model employs a radial basis
212 function (RBF) kernel [34] with added noise and is allowed to update its hyperparameters and restart the
213 process up to 200 times on each outer fold of the training data. Unlike most other models, it does not update
214 these hyperparameters using nested cross validation nor the Tree-Structured Parzen Estimator method [30]
215 but instead an internal process which maximizes the log-marginal likelihood [34]. The model’s accuracy was
216 determined using basic (non-nested) five-fold cross validation.

217 Neural network models are based on the structure of neural networks found in the brain [25]. They
218 consist of layers of interconnected “neurons” which can process and transmit information. Each neuron
219 receives the inputs from the previous layer and performs a weighted sum on these inputs, applies a bias,
220 and passes it through a nonlinear activation function to produce an output for the next layer of neurons.
221 Adjusting these weights and biases (through training the model) allows a sufficiently large neural network
222 to approximate arbitrary functional relationships [18]. However, since neural networks use many weights
223 and biases to fit the data, they are prone to over-fitting and lack interpretability. Many neural network
224 architectures exist in the literature with a variety of strengths and weaknesses. After testing many different
225 architectures and techniques, a simplified DenseNet architecture [15, 35] was used in this study due to its
226 feature-reuse capabilities (*i.e.*, inputs are not “lost” as the depth of the neural network increases). The neural
227 network model also employs dropout regularization [36] and k -fold averaging [27] to reduce overfitting.

228 3. 2SLGG Muzzle Velocity Prediction Results and Discussion

229 Linear least-squares (basic, LASSO, ridge, and elastic-net), support vector, Gaussian process, and artificial
230 neural network regression were used to empirically model the 2SLGG’s muzzle velocity. The independent
231 variables (parameters) used were (1) projectile package mass, (2) primary powder mass, (3) secondary powder
232 mass, (4) pump tube fill (working gas) pressure, (5) tankage (backfill) pressure, (6) piston mass, (7)

233 burst disk score depth, (8) piston fit tightness, (9) number of volume reducers in the powder breech, and
 234 (10) gunpowder type. The results of each regression model and their comparison to those from two numeri-
 235 cal models (PCLGGP and LGGUN) are presented in this section. The models are compared based on the
 236 root-mean-squared error (RMSE):

$$RMSE = \sqrt{\frac{1}{n} \sum_{i=1}^n |f(\vec{x}_i) - y_i|^2}, \quad (5)$$

237 where n is the number of (\vec{x}_i, y_i) input(s)/output pairs to the regression model $f(\vec{x}_i)$. RMSE (Eq. 5)
 238 approximates the standard deviation of the errors (lower is better). All predictions and error measurements
 239 are based on data points withheld during the training process.

240 3.1. Regression Results for 2SLGG Muzzle Velocity Predictions

241 The predicted projectile velocity obtained using the most basic model (linear regression) was compared to
 242 that from PCLGGP (Charters' code) over the given 2SLGG velocity range 1.5-6.8 km/s. The linear model
 243 (RMSE = 0.260 km/s) matched the measured muzzle velocity values (diagonal dashed line) significantly
 244 better than the PCLGGP model predictions (RMSE = 0.597 km/s) especially at lower muzzle velocities
 245 (Figure 4a). The plot clearly shows that PCLGGP consistently over-predicted the actual values at lower
 246 launch velocities (*i.e.*, <5.0 km/s) but yielded more accurate results for velocities >5 km/s. Since Char-
 247 ter's code does not account for the effect of piston and projectile friction, the PCLGGP model has been
 248 reported to consistently over-predict muzzle velocities by 10–20% [37]. Since these effects become less sig-
 249 nificant for more energetic shots, the PCLGGP model error will tend to decrease with increasing muzzle
 250 velocity. The difference between PCLGGP and linear regression is clearer in Figure 4b, which shows the
 251 velocity normalized absolute error ($\bar{\epsilon} = |v_{measured} - v_{predicted}|/v_{measured}$) compared to the measured veloc-
 252 ity. PCLGGP's relative error exceeded 70% at lower velocities (~ 2 km/s) but significantly improved with
 253 increasing projectile velocity. The linear model predicted a few outliers at lower velocities but provided more
 254 stable predictions throughout the entire velocity range. The dashed lines in Figure 5b demonstrate that the
 255 average relative error for the linear regression predictions (5.4%) was dramatically lower than those for the
 256 PCLGGP model (15.8%).

257 The results of LASSO (RMSE = 0.259 km/s), ridge (RMSE = 0.260 km/s), and elastic-net (RMSE =
 258 0.260 km/s) regression were almost identical to the linear regression results. In all cases, the penalty terms
 259 were negligibly small. Recall that with a null penalty term the LASSO, ridge, and elastic-net regression
 260 predictions will be identical to that for basic linear regression with no reduction in overfitting. Hence, a
 261 penalty term near zero implies that, for a comparable linear model, there is little to no benefit in removing
 262 any independent variables. The support vector regression (RMSE = 0.263 km/s) predictions approach,
 263 but do not improve upon, the linear model results even with significant hyperparameter tuning. Hence,
 264 the support vector regression model was the only model considered that performed *worse* than basic linear
 265 regression. A summary of all model results is presented in order of descending RMSE values in Table 2.

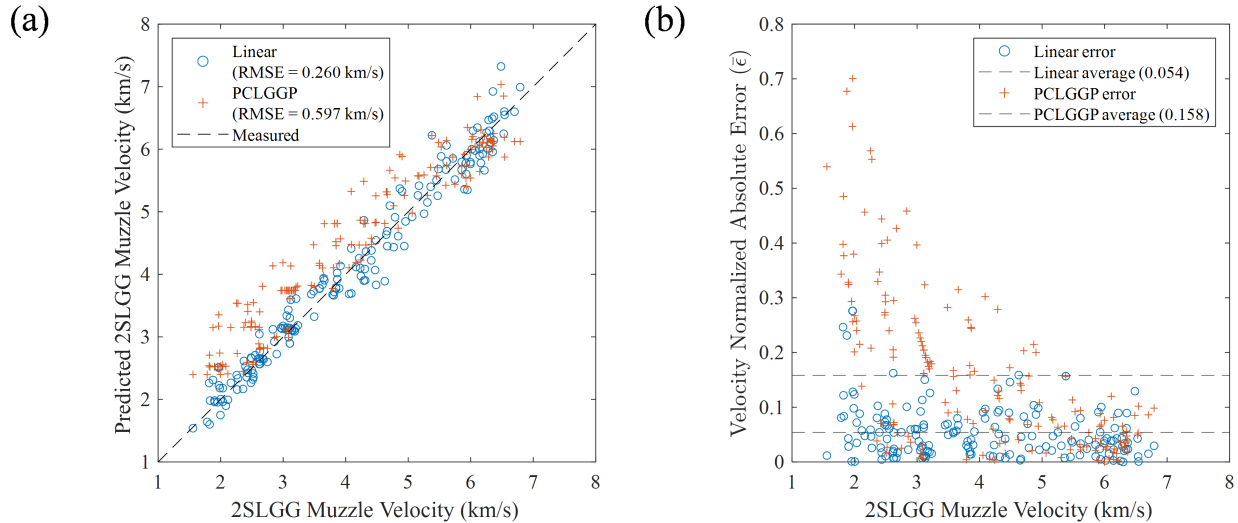


Figure 4: PCLGGP (Charters’ code) results compared to linear regression results: (a) predicted muzzle velocity versus measured muzzle velocity and (b) normalized absolute error versus measured muzzle velocity.

266 A reasonable explanation exists as to why the LASSO, ridge, elastic-net, and support vector methods
 267 did not perform better than simple linear regression. While 171 2SLGG launches are significant from a
 268 cost and time standpoint, there are still relatively few data points for regression, especially when using
 269 10 independent variables. Furthermore, significant random error between nearly identical shots makes it
 270 difficult to differentiate trends in the data from random noise. For example, when linear regression was
 271 performed with the secondary powder mass as the only independent variable, the model achieved an RMSE
 272 of 0.439 km/s and an R-squared value of 0.92 (*i.e.*, 92% of all the variance in the data can be explained
 273 solely by the secondary powder mass). The coupled effects of other variables are likely numerous, complex,
 274 and largely overshadowed by random error and the dominant effect of the secondary powder mass. This
 275 makes it more difficult to model weaker trends without overfitting the limited data.

276 Gaussian process regression showed a noticeable improvement (RMSE = 0.240 km/s) over linear regres-
 277 sion (RMSE = 0.260 km/s). Moreover, it also gives an estimate of the variance in the prediction at any
 278 evaluated point—this is useful in determining the model’s confidence in each prediction. The linear, LASSO,

Table 2: The root-mean-square error (RMSE) over holdout data for each model over the 2SLGG operational velocity range 1.5-6.8 km/s (The Quad. RMSE column represents the results when quadratic features were passed through the model). LGGUN results (*) correspond to a different set of experiments performed using multiple 2SLGGs [38, 39].

| No. | Model | RMSE (km/s) | Quad. RMSE (km/s) |
|-----|-------------------------|-------------|-------------------|
| 1 | PCLGGP (Charters’ code) | 0.597 | ... |
| 2 | LGGUN [38, 39] | 0.302* | ... |
| 3 | Support Vector | 0.263 | ... |
| 4 | Linear | 0.260 | 1.445 |
| 5 | Elastic-Net | 0.260 | 0.255 |
| 6 | Ridge | 0.260 | 0.249 |
| 7 | LASSO | 0.259 | 0.248 |
| 8 | Gaussian Process | 0.240 | ... |
| 9 | Neural Network | 0.234 | ... |

279 ridge, and elastic-net methods were also expanded to quadratic regression by using a quadratic expansion
280 of the variables. The basic quadratic model (linear regression model with quadratic variables) performed
281 significantly worse (RMSE = 1.445 km/s) than basic linear regression. In contrast, the quadratic LASSO,
282 ridge, and elastic-net models provided a *slight* improvement in prediction error (RMSE = 0.248-0.255 km/s)
283 relative to basic linear regression (RMSE = 0.260 km/s; *cf.*, Table 2). The difference between the basic
284 quadratic model results and the results of the quadratic LASSO, ridge, and elastic-net models is explained
285 by the lack of weight (coefficient) regularization in basic polynomial regression, where the coefficients of all
286 polynomial terms must be determined, leading to substantial overfitting in higher order regression as the
287 number of terms increases. In contrast, the LASSO, ridge, and elastic-net regression techniques can eliminate
288 excess (non-contributing) variables to avoid overfitting. Moreover, since the RMSE is calculated based on
289 unseen data (instead of the training data), the overfitted basic quadratic model performed much worse than
290 the basic linear model. Note that the RMSE values of the quadratic models were all *greater* than that for
291 the Gaussian process model (RMSE = 0.240 km/s).

292 In contrast, the neural network model (RMSE = 0.234 km/s) was the most accurate of all regression
293 models considered and exhibited reliable (albeit nominal) improvement over linear regression (RMSE =
294 0.260 km/s) and Gaussian process regression (RMSE = 0.240 km/s). Figure 5a compares the linear and
295 neural network predictions to measured velocities, and Figure 5b compares the relative error of the linear
296 and neural network predictions at different muzzle velocities. In both Figure 5a and Figure 5b, the modest
297 improvements in predicted launch velocities obtained using the neural network model are readily apparent
298 but are much less pronounced than the differences between PCLGGP and linear regression predictions shown
299 in Figure 4. Moreover, error histograms corresponding to the neural network and PCLGGP results (Figure 6)
300 clearly show that the neural network model's error distribution has a lower standard deviation and less bias
301 towards over-prediction. As an aside, as the number of experiments is further increased, the accuracy of
302 the neural network and Gaussian process models are expected to increase dramatically relative to the other
303 regression models considered here since they are well suited for approximating the nonlinear relationships
304 between independent variables that a larger data set would reveal. As the number of experiments increases,
305 however, the neural network model will scale better with the size of the data set.

306 Despite the neural network model's relative increase in accuracy and potential for improved predictions
307 on larger data sets, it has some unavoidable limitations relative to the other empirical models. For example,
308 in traditional polynomial regression, the magnitude and sign of each coefficient in the fitted model defines the
309 influence of each independent variable (projectile package mass, working gas pressure, *etc.*) on the predicted
310 response (*i.e.*, projectile velocity), as well as how coupled interactions between independent variables affect
311 the model outputs. The neural network model, however, lacks such intuition. Relationships between inputs
312 and outputs can be estimated by evaluating the neural network model at different points, but not directly
313 interpreted from the trained weights and biases. Similarly, while the Gaussian process model was slightly
314 less accurate than the neural network model, it provides a prediction of uncertainty that the neural network

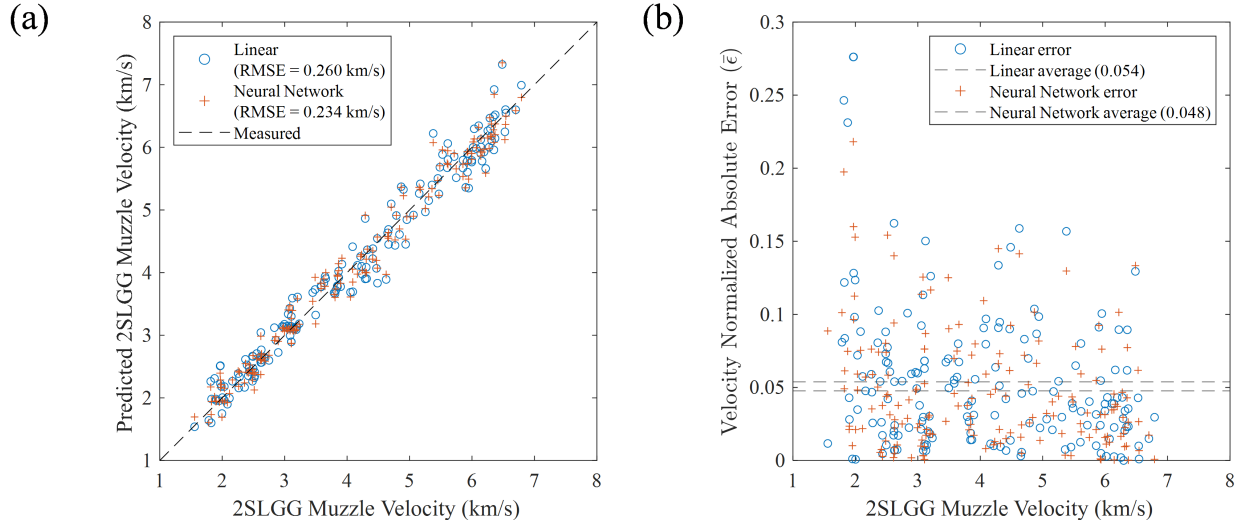


Figure 5: Neural network model results compared to linear results: (a) predicted muzzle velocity versus measured muzzle velocity and (b) velocity normalized absolute error versus measured muzzle velocity.

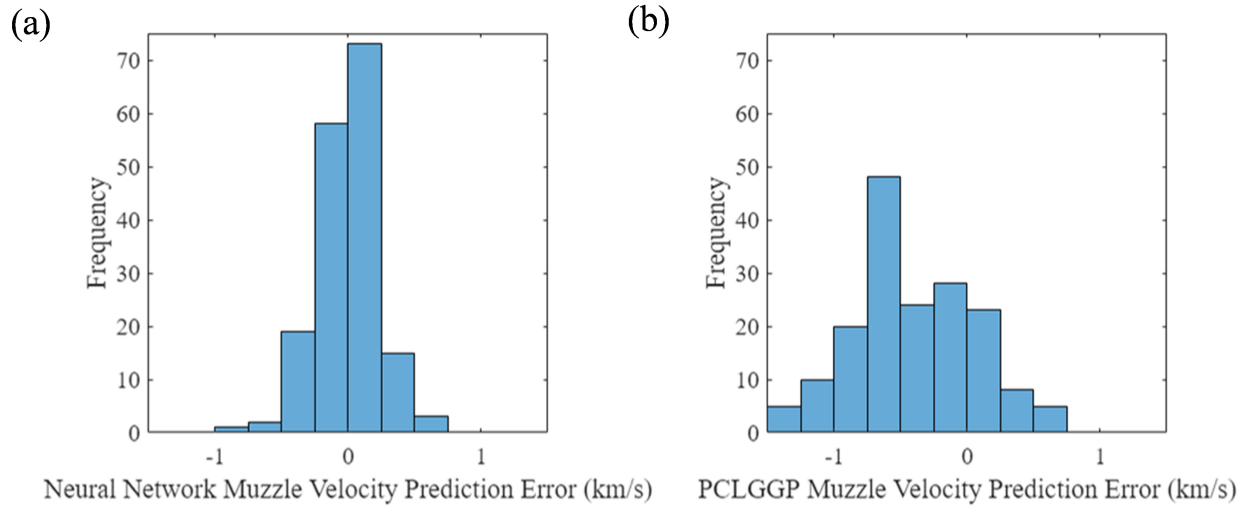


Figure 6: Histogram of errors for (a) the neural network model and (b) the PCLGGP predictions. Over-predictions by the model are represented as negative to match $y = \hat{y} + \epsilon$.

315 model cannot. The slight loss of accuracy associated with use of the Gaussian process model may be offset
 316 by the ability to estimate prediction uncertainty. Overall, most of the regression methods considered in this
 317 study had an RMSE value *less than one-half* that for the PCLGGP model. This demonstrates that even
 318 simple empirical models are well-suited for predicting 2SLGG muzzle velocity if sufficient experimental data
 319 exists.

320 3.2. Projectile Velocity Absolute Error Percentiles and Comparison to LGGUN

321 Using data from the 171 TAMU HVIL 2SLGG experiments with muzzle velocities in the range 1.5-
 322 6.8 km/s, projectile velocity error estimates obtained using the PCLGGP model and 11 regression models

323 were expressed in terms of absolute error percentiles. For example, the 50th percentile (2nd quartile, Q2)
324 would define the *median absolute error* associated with each model. Similarly, the absolute error associated
325 with the 25th percentile (1st quartile, Q1) means that 25% of the predicted values would have absolute errors
326 less than or equal to the specified value. Hence, absolute error percentiles can be used to assess how well a
327 given model approximates the actual velocity over the entire range of experimental observations and estimate
328 the likelihood of different magnitudes of error in future predictions. The absolute error estimates generated
329 using the 171 TAMU 2SLGG experiments in this study were compared to published values predicted using
330 LGGUN [8] for 52 experiments performed using five *different* 2SLGGs over a velocity range of 3-11 km/s [38,
331 39]. As mentioned previously, LGGUN is a leading edge 2SLGG performance prediction code.

332 Excluding the basic quadratic model (*i.e.*, linear regression model with quadratic variables), all of the
333 regression models' root mean square error (RMSE) values (0.234-0.263 km/s) were *lower* than that for the
334 LGGUN model (0.302 km/s; *cf.*, Table 2). Similarly, Table 3 includes a summary of predicted velocity
335 absolute error estimates corresponding to the 25th, 50th, 75th, and 100th percentiles (*i.e.*, quartiles Q1, Q2,
336 Q3, Q4, respectively) for the PCLGGP and 11 regression models, as well as generic LGGUN values from
337 data provided by D. W. Bogdanoff and shown in the literature [38, 39]. Figure 7 contains a graphical
338 representation of these same data using "box and whisker" plots [40]. For a given model, the "box" provides
339 the Q1, Q2 (median), and Q3 velocity absolute error estimates, as suggested in the figure. The "whiskers"
340 associated with a given model defines the minimum (Q0) and maximum (Q4) values including outliers. Not
341 surprisingly, the absolute errors associated with LGGUN predictions were over 40% lower than those for
342 PCLGGP for all quartiles. Similarly, all of the regression models significantly outperformed the PCLGGP
343 model. For example, the median absolute error (50th percentile; Q2) for each of the regression models was
344 at least 62% lower than the PCLGGP value. With the exception of the 100th percentile (Q4) absolute
345 error for the basic quadratic linear model, all of the regression models outperformed Charters' code over
346 the entire range of experiments. The regression model Q1-Q3 absolute errors from the TAMU 2SLGG
347 experiments also compared favorably to general absolute error estimates obtained using LGGUN. Excluding
348 the basic quadratic linear model, the 25th (Q1), 50th (Q2, median), and 75th percentile (Q3) absolute errors
349 for the regression models were at least 10%, 25%, and 30% *lower* than the corresponding LGGUN values,
350 respectively. For comparison purposes, the neural network model's predicted 25th, 50th, and 75th percentile
351 absolute errors were 18%, 39%, and 38% lower than the generic LGGUN values, respectively. All of the
352 regression model absolute errors, however, *exceeded* the LGGUN 100th percentile (Q4) value. This latter
353 difference may be attributable to a number of factors including: 1) the increased likelihood of encountering
354 outliers within the larger TAMU dataset (171 experiments) compared to the dataset used to validate LGGUN
355 (52 experiments); 2) the reliance of regression models on data points in the training set with similar or
356 "nearby" inputs (*i.e.*, experiments conducted at the extreme range of independent variables will be more
357 difficult to predict), and 3) better fidelity over the entire range of independent variables associated with
358 the physics-based LGGUN numerical model. As an aside, if LGGUN was used to predict muzzle velocities

Table 3: Absolute error percentiles (in km/s) for all considered models. LGGUN results (*) correspond to a different set of experiments performed using multiple 2SLGGs [38, 39].

| No. | Model | Absolute error Percentile (Quartile) | | | |
|--------------------------|-------------------|--------------------------------------|---------------------------------|---------------------------------|----------------------------------|
| | | 25 th (Q1) (km/s) | 50 th (Q2) (km/s) | 75 th (Q3) (km/s) | 100 th (Q4) (km/s) |
| <i>Numerical Models</i> | | | | | |
| 1 | PCLGGP | 0.185 | 0.501 | 0.677 | 1.381 |
| 2 | LGGUN [38, 39] | 0.083* | 0.226* | 0.395* | 0.655* |
| <i>Regression Models</i> | | | | | |
| 3 | Linear | 0.065 | 0.168 | 0.250 | 0.844 |
| 4 | Quad. Linear | 0.083 | 0.192 | 0.377 | 11.686 |
| 5 | Ridge | 0.065 | 0.168 | 0.247 | 0.839 |
| 6 | Quad. Ridge | 0.058 | 0.139 | 0.269 | 1.162 |
| 7 | LASSO | 0.068 | 0.155 | 0.261 | 0.826 |
| 8 | Quad. LASSO | 0.065 | 0.142 | 0.246 | 1.168 |
| 9 | Elastic-Net | 0.065 | 0.163 | 0.256 | 0.833 |
| 10 | Quad. Elastic-Net | 0.073 | 0.151 | 0.257 | 1.062 |
| 11 | Support Vector | 0.074 | 0.156 | 0.264 | 0.903 |
| 12 | Gaussian Process | 0.069 | 0.145 | 0.255 | 0.992 |
| 13 | Neural Network | 0.068 | 0.138 | 0.244 | 0.865 |

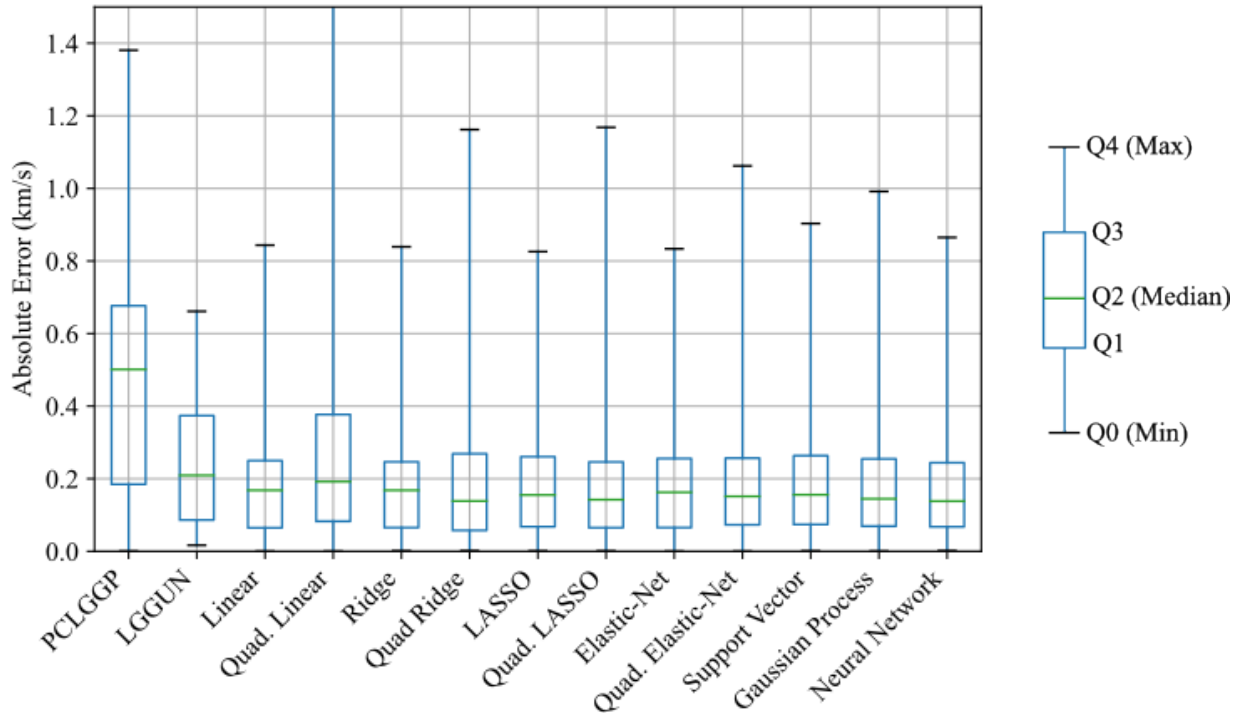


Figure 7: Box and whisker plots of the prediction absolute error for PCLGGP, LGGUN, and all considered regression models. Note that the Q4 whisker plot for the Quad. Linear model was cutoff since the Q4 value was much larger than that for any other model. LGGUN results correspond to a different set of experiments performed using multiple 2SLGGs [38, 39].

359 for the 171 experiments using TAMU 2SLGG launch parameters, the predicted absolute error values would
360 likely improve upon the LGGUN values reported here. Nonetheless, these results suggest that easy-to-
361 implement, maintain, and scalable regression models may provide an attractive alternative to more complex
362 computational models such as PCLGGP and LGGUN for 2SLGG launch velocity predictions. While LGGUN
363 can provide crucial information about shock formation, bore erosion, pump tube pressure-time histories, and
364 other key aspects of specific 2SLGG performance, model specification and interpretation of results requires
365 considerable expertise. Clearly, regression models that are amenable to scaling across different 2SLGG
366 platforms can augment physics-based numerical models, particularly as the volume of available experimental
367 data increases. The regression models, such as Gaussian process and neural network, have the potential to
368 markedly improve predictive capabilities, identify complex coupling between experimental parameters, and
369 reduce uncertainty. In the future, it may be possible to significantly reduce the maximum (Q4) absolute
370 errors using *physics-informed* neural network models or Gaussian process regression models [41].

371 4. Conclusions and Future Work

372 In this study, linear, ridge, LASSO, elastic-net, support vector, Gaussian process, and neural network
373 regression models were developed to predict two-stage light gas gun (2SLGG) projectile velocities as a
374 function of 10 independent variables (launch parameters): (1) projectile package mass, (2) primary powder
375 mass, (3) secondary powder mass, (4) pump tube fill (working gas) pressure, (5) tankage (backfill) pressure,
376 (6) piston mass, (7) burst disk score depth, (8) piston fit tightness, (9) number of volume reducers in the
377 powder breech, and (10) gunpowder type. The models were fitted to and validated against performance data
378 from 171 experiments (projectile velocities, 1.5-6.8 km/s) conducted using a powder-driven 12.7 mm bore
379 2SLGG at the Texas A&M University Hypervelocity Impact Lab (TAMU HVIL). Regression model muzzle
380 velocity estimates for all 171 shots were compared to numerical predictions obtained using the physics-based
381 Piston Compression Light Gas Gun Performance (PCLGGP) software package (*i.e.*, “Charters’ code”). In
382 addition, the prediction absolute error distributions from the regression and PCLGGP models were compared
383 to independent values determined using the cutting-edge, physics-based LGGUN code for a different set of
384 experiments involving multiple 2SLGGs.

385 Except for the basic quadratic model (*i.e.*, linear regression model with quadratic variables), all of the
386 regression models significantly outperformed Charters’ code over the entire range of experiments. Their root
387 mean square error (RMSE) values (0.234-0.263 km/s) were significantly lower than that for the PCLGGP
388 model (0.597 km/s), and their predicted absolute error distributions were clearly superior to that for Charter’s
389 code. The median absolute error (50th percentile) for each of the regression models was at least 62% lower
390 than the PCLGGP value. In general, there was not a significant difference between simple linear regression
391 (RMSE = 0.260 km/s) and the other regression models. Gaussian process regression (RMSE = 0.240 km/s),
392 however, includes an estimate of prediction confidence. The neural network model (RMSE = 0.234 km/s)
393 was the most accurate regression technique considered and is particularly well-suited to scale with large data

394 sets.

395 Not surprisingly, the absolute errors associated with independent LGGUN predictions were at least
396 40% lower than those for PCLGGP for all percentiles. Interestingly, the regression model results from the
397 TAMU 2SLGG experiments compared favorably to LGGUN results. Excluding the basic quadratic model,
398 the regression models' root mean square error (RMSE) values (0.234-0.263 km/s) were lower than that for
399 the LGGUN model (0.302 km/s). Similarly, the corresponding 25th-75th percentile absolute errors for the
400 regression models were significantly lower than corresponding LGGUN values. LGGUN, however, predicted
401 a lower maximum (100th percentile) absolute error than any regression model. In general, regression models
402 may not perform as well as physics-based computational models in predicting individual experimental results
403 involving extreme values of independent variables. In the future, this limitation can be remedied, in part,
404 using physics-informed neural network or Gaussian process models [41] that incorporate both prior data and
405 general physics-based knowledge over the domain.

406 This study demonstrates that straightforward regression models may provide an attractive alternative
407 to more complex deterministic models for 2SLGG launch velocity predictions. Regression models that
408 are amenable to scaling across different 2SLGG platforms can augment physics-based numerical models
409 (particularly as the volume of available experimental data increases) and have the potential to markedly
410 improve predictive capabilities, identify complex coupling between experimental parameters, and reduce
411 uncertainty.

References

- [1] M. I. Allende, J. E. Miller, B. A. Davis, E. L. Christiansen, M. D. Lepech, D. J. Loftus, Prediction of micrometeoroid damage to lunar construction materials using numerical modeling of hypervelocity impact events, *International Journal of Impact Engineering* 138 (2020) 103499.
- [2] J. A. Rogers, N. Bass, P. T. Mead, A. Mote, G. D. Lukasik, M. Intardonato, K. Harrison, J. D. Leaverton, K. R. Kota, J. W. Wilkerson, J. N. Reddy, W. D. Kulatilaka, T. E. Lacy, The texas a&m university hypervelocity impact laboratory: A modern aeroballistic range facility, *Review of Scientific Instruments* 93 (2022) 085106.
- [3] J. Rogers, N. Bass, M. Wiest, Z. Wantz, J. Wilkerson, T. Lacy, The pursuit of hypervelocities: A review of two-stage light gas gun aeroballistic ranges, *International Journal of Impact Engineering* 185 (2024) 104861.
- [4] A. C. Charters, B. P. Denardo, V. J. Rossow, Development of a piston-compressor type light-gas gun for the launching of free-flight models at high velocity, Technical Report, 1957.
- [5] R. J. Rynearson, J. L. Rand, Optimization of a two stage light gas gun, Technical Report, 1972.

- [6] R. Piacesi, D. F. Gates, A. E. Seigel, Computer analysis of two-stage hypervelocity model launchers, Technical Report, 1963.
- [7] D. W. Bogdanoff, R. J. Miller, New higher-order Godunov code for modelling performance of two-stage light gas guns, Technical Report, 1995.
- [8] D. W. Bogdanoff, LGGUN User's Manual, 2020.
- [9] B. Lexow, M. Wickert, K. Thoma, F. Schäfer, M. H. Poelchau, T. Kenkmann, The extra-large light-gas gun of the fraunhofer emi: Applications for impact cratering research, *Meteoritics & Planetary Science* 48 (2013) 3–7.
- [10] B. Lexow, A. Bueckle, M. Wickert, S. Hiermaier, The xllgg—a hypervelocity launcher for impact cratering research., *Bridging the Gap III: Impact Cratering In Nature, Experiments, and Modeling* 1861 (2015) 1046.
- [11] P. Shojaei, M. Trabia, B. O'Toole, R. Jennings, Predicting the projectile velocity of a two-stage gas gun using machine learning, volume 86168, 2022, p. V003T05A014.
- [12] L. Breiman, Random forests, *Machine learning* 45 (2001) 5–32.
- [13] W. D. Crozier, W. Hume, High-velocity, light-gas gun, *Journal of Applied Physics* 28 (1957) 892–894.
- [14] H. F. Swift, *Light-gas gun technology: a historical perspective*, Springer-Verlag Berlin Heidelberg, Germany, 2005, p. 1–36.
- [15] D. Chen, F. Hu, G. Nian, T. Yang, Deep residual learning for nonlinear regression, *Entropy* 22 (2020) 193.
- [16] A. J. Smola, B. Schölkopf, A tutorial on support vector regression, *Statistics and computing* 14 (2004) 199–222.
- [17] C. E. Rasmussen, Evaluation of Gaussian processes and other methods for non-linear regression, Technical Report, 1997.
- [18] K. Hornik, M. Stinchcombe, H. White, Multilayer feedforward networks are universal approximators, *Neural networks* 2 (1989) 359–366.
- [19] C. A. Micchelli, Y. Xu, H. Zhang, Universal kernels., *Journal of Machine Learning Research* 7 (2006).
- [20] T. N. Canning, C. S. James, A. Seiff, Ballistic range technology(conference on ballistic range techniques and equipment) (1970).
- [21] H. F. Swift, D. E. Strange, Sabot discard technology, Physics Applications Inc., Internal Report (1987).

- [22] Extruded Rifle Powders Safety Data Sheet, Technical Report, 2019.
- [23] Single Base Powders Safety Data Sheet, Technical Report, 2022.
- [24] Shooters World Reloading Data, Technical Report, 2019.
- [25] G. James, D. Witten, T. Hastie, R. Tibshirani, J. Taylor, An introduction to statistical learning: With applications in python, Springer, 2023.
- [26] S. Ruder, An overview of gradient descent optimization algorithms, arXiv preprint arXiv:1609.04747 (2016).
- [27] Y. Jung, J. Hu, Ak-fold averaging cross-validation procedure, Journal of nonparametric statistics 27 (2015) 167–179.
- [28] O. Sagi, L. Rokach, Ensemble learning: A survey, Wiley Interdisciplinary Reviews: Data Mining and Knowledge Discovery 8 (2018) e1249.
- [29] J. Wainer, G. Cawley, Nested cross-validation when selecting classifiers is overzealous for most practical applications, Expert Systems with Applications 182 (2021) 115222.
- [30] J. Bergstra, D. Yamins, D. Cox, Making a science of model search: Hyperparameter optimization in hundreds of dimensions for vision architectures, 2013, p. 115–123.
- [31] R. Tibshirani, Regression shrinkage and selection via the lasso, Journal of the Royal Statistical Society: Series B (Methodological) 58 (1996) 267–288.
- [32] A. E. Hoerl, R. W. Kennard, Ridge regression: Biased estimation for nonorthogonal problems, Technometrics 12 (1970) 55–67.
- [33] H. Zou, T. Hastie, Regularization and variable selection via the elastic net, Journal of the royal statistical society: series B (statistical methodology) 67 (2005) 301–320.
- [34] F. Pedregosa, G. Varoquaux, A. Gramfort, V. Michel, B. Thirion, O. Grisel, M. Blondel, P. Prettenhofer, R. Weiss, V. Dubourg, J. Vanderplas, A. Passos, D. Cournapeau, M. Brucher, M. Perrot, E. Duchesnay, Scikit-learn: Machine learning in python, Journal of Machine Learning Research 12 (2011) 2825–2830.
- [35] G. Huang, Z. Liu, L. Van Der Maaten, K. Q. Weinberger, Densely connected convolutional networks, 2017, p. 4700–4708.
- [36] N. Srivastava, G. Hinton, A. Krizhevsky, I. Sutskever, R. Salakhutdinov, Dropout: a simple way to prevent neural networks from overfitting, The journal of machine learning research 15 (2014) 1929–1958.
- [37] A. C. Charters, D. K. Sangster, Fortran computer program for interior ballistic analysis of light-gas guns, Informal Manual available from Dr. Charters (1973).

- [38] D. W. Bogdanoff, Further Validation of a CFD Code for Calculating the Performance of Two-Stage Light Gas Guns, Technical Report, 2017.
- [39] D. W. Bogdanoff, Private communication regarding individual data points plotted in figure 17 in ref. [38], 2023.
- [40] S. H. C. DuToit, A. G. W. Steyn, R. H. Stumpf, Graphical exploratory data analysis, Springer Science & Business Media, 2012.
- [41] G. Pang, G. E. Karniadakis, Physics-informed learning machines for partial differential equations: Gaussian processes versus neural networks, *Emerging Frontiers in Nonlinear Science* (2020) 323–343.

Appendix A: Experimental data

Table A.1: Experimental 2SLGG loading parameters used in regression model training and validation, as well as *measured* muzzle velocity for reference.

| Projectile Package Mass (g) | Primary Powder Mass (g) | Secondary Powder Mass (g) | Burst Disc Score Depth (in) | Piston Mass (g) | Target Tank Pres- sure (Torr) | Pump Tube Pres- sure (psi) | Volume Re- ducers | Piston Tightness | H4831SC | IMR 4831 | Projectile Velocity (m/s) |
|-----------------------------------|-------------------------------|---------------------------------|-----------------------------------|--------------------|-------------------------------------|----------------------------------|----------------------|---------------------|---------|----------|---------------------------------|
| 6.083 | 1.420 | 100.2 | 0.020 | 364.4 | 200 | 140 | 1 | 0.50 | 0 | 0 | 4165 |
| 3.381 | 1.401 | 100.5 | 0.020 | 362.6 | 200 | 140 | 1 | 0.50 | 0 | 0 | 4665 |
| 3.387 | 1.511 | 100.0 | 0.020 | 365.3 | 200 | 140 | 1 | 0.50 | 0 | 0 | 4938 |
| 3.388 | 1.745 | 101.0 | 0.020 | 367.1 | 200 | 279 | 1 | 0.50 | 0 | 0 | 3847 |
| 3.372 | 1.751 | 100.1 | 0.020 | 363.8 | 200 | 279 | 1 | 0.50 | 0 | 0 | 4091 |
| 3.389 | 1.751 | 130.0 | 0.020 | 363.6 | 200 | 140 | 1 | 0.50 | 0 | 0 | 5615 |
| 3.382 | 1.754 | 120.1 | 0.020 | 363.7 | 200 | 141 | 1 | 0.50 | 0 | 0 | 5359 |
| 3.389 | 1.749 | 110.1 | 0.020 | 365.4 | 200 | 161 | 1 | 0.50 | 0 | 0 | 4956 |
| 2.315 | 1.743 | 100.1 | 0.020 | 363.9 | 200 | 280 | 1 | 0.50 | 0 | 0 | 4486 |
| 3.379 | 1.753 | 110.7 | 0.020 | 437.7 | 200 | 160 | 1 | 0.50 | 0 | 0 | 5253 |
| 3.385 | 1.751 | 150.1 | 0.020 | 363.8 | 200 | 200 | 1 | 0.50 | 0 | 0 | 6035 |
| 3.379 | 1.753 | 150.1 | 0.020 | 366.6 | 250 | 220 | 1 | 0.50 | 0 | 0 | 5612 |
| 3.379 | 1.753 | 150.5 | 0.020 | 365.7 | 250 | 200 | 1 | 0.50 | 0 | 0 | 5379 |
| 6.059 | 1.751 | 100.4 | 0.020 | 761.7 | 250 | 200 | 1 | 0.50 | 0 | 0 | 4215 |
| 3.387 | 1.753 | 100.0 | 0.020 | 366.2 | 200 | 279 | 1 | 0.50 | 0 | 0 | 3488 |
| 6.029 | 1.755 | 100.0 | 0.020 | 767.2 | 200 | 200 | 1 | 0.50 | 0 | 0 | 4324 |
| 6.055 | 1.751 | 100.8 | 0.020 | 763.7 | 200 | 200 | 1 | 0.50 | 0 | 0 | 4413 |
| 2.163 | 1.757 | 120.0 | 0.020 | 363.1 | 200 | 174 | 1 | 0.50 | 0 | 0 | 5946 |
| 2.161 | 1.747 | 60.2 | 0.020 | 363.5 | 200 | 249 | 1 | 0.50 | 0 | 0 | 2277 |
| 3.391 | 1.750 | 100.0 | 0.020 | 363.5 | 200 | 139 | 1 | 0.50 | 0 | 0 | 4483 |
| 3.397 | 1.747 | 110.0 | 0.020 | 363.2 | 197 | 160 | 1 | 0.50 | 0 | 0 | 4290 |
| 3.400 | 1.749 | 120.1 | 0.020 | 363.6 | 252 | 140 | 1 | 0.50 | 0 | 0 | 5470 |
| 3.399 | 1.747 | 120.2 | 0.020 | 363.6 | 250 | 200 | 1 | 0.50 | 0 | 0 | 4789 |
| 2.141 | 1.750 | 150.0 | 0.020 | 363.1 | 200 | 221 | 1 | 0.50 | 0 | 0 | 6527 |
| 2.158 | 1.764 | 150.0 | 0.020 | 362.8 | 200 | 220 | 1 | 0.50 | 0 | 0 | 6107 |

Table A.1: Experimental 2SLGG loading parameters used in regression model training and validation, as well as *measured* muzzle velocity for reference.

| Projectile Package Mass (g) | Primary Powder Mass (g) | Secondary Powder Mass (g) | Burst Disc Score Depth (in) | Piston Mass (g) | Target Tank Pres- sure (Torr) | Pump Tube Pres- sure (psi) | Volume Re- ducers | Piston Tightness | H4831SC | IMR 4831 | Projectile Velocity (m/s) |
|-----------------------------------|-------------------------------|---------------------------------|-----------------------------------|--------------------|-------------------------------------|----------------------------------|----------------------|---------------------|---------|----------|---------------------------------|
| 3.379 | 1.746 | 100.0 | 0.020 | 363.8 | 200 | 271 | 1 | 0.50 | 0 | 0 | 3844 |
| 3.394 | 1.757 | 60.0 | 0.020 | 363.5 | 200 | 249 | 1 | 0.50 | 0 | 0 | 2485 |
| 6.036 | 1.745 | 60.1 | 0.020 | 363.5 | 200 | 250 | 1 | 0.50 | 0 | 0 | 1900 |
| 6.039 | 1.760 | 60.1 | 0.020 | 363.4 | 200 | 250 | 1 | 0.50 | 0 | 0 | 2035 |
| 2.081 | 1.751 | 60.0 | 0.020 | 363.5 | 202 | 250 | 1 | 0.50 | 0 | 0 | 2524 |
| 3.400 | 1.749 | 150.0 | 0.020 | 363.5 | 201 | 221 | 1 | 0.50 | 0 | 0 | 6142 |
| 3.386 | 1.749 | 150.1 | 0.020 | 363.9 | 76 | 221 | 1 | 0.50 | 0 | 0 | 6372 |
| 6.033 | 1.748 | 60.4 | 0.020 | 364.1 | 199 | 249 | 1 | 0.50 | 0 | 0 | 2003 |
| 3.399 | 1.751 | 150.0 | 0.020 | 363.2 | 75 | 220 | 1 | 0.50 | 0 | 0 | 6342 |
| 6.035 | 1.757 | 60.2 | 0.020 | 364.0 | 199 | 249 | 1 | 0.50 | 0 | 0 | 2083 |
| 3.399 | 1.751 | 60.0 | 0.020 | 363.5 | 199 | 249 | 1 | 0.50 | 0 | 0 | 2163 |
| 6.055 | 1.750 | 60.0 | 0.020 | 363.5 | 199 | 250 | 1 | 0.50 | 0 | 0 | 1829 |
| 6.040 | 1.750 | 60.2 | 0.020 | 363.9 | 203 | 250 | 1 | 0.50 | 0 | 0 | 1953 |
| 6.042 | 1.750 | 60.0 | 0.020 | 363.9 | 199 | 249 | 1 | 0.50 | 0 | 0 | 1905 |
| 3.401 | 1.751 | 150.0 | 0.020 | 363.6 | 76 | 200 | 1 | 0.50 | 0 | 0 | 6537 |
| 2.099 | 1.750 | 60.0 | 0.020 | 363.7 | 199 | 251 | 1 | 0.50 | 0 | 0 | 2256 |
| 3.387 | 1.750 | 150.0 | 0.020 | 363.9 | 75 | 250 | 1 | 0.50 | 0 | 0 | 6295 |
| 3.382 | 1.750 | 145.0 | 0.020 | 363.8 | 75 | 220 | 1 | 0.50 | 0 | 0 | 6253 |
| 3.399 | 1.749 | 125.0 | 0.020 | 363.0 | 90 | 220 | 1 | 0.50 | 0 | 1 | 5855 |
| 2.135 | 1.748 | 165.0 | 0.020 | 364.0 | 100 | 250 | 1 | 0.50 | 0 | 1 | 6484 |
| 2.145 | 1.758 | 125.0 | 0.020 | 364.2 | 85 | 220 | 1 | 0.50 | 0 | 1 | 6162 |
| 6.048 | 1.750 | 60.0 | 0.020 | 363.2 | 200 | 250 | 1 | 1.00 | 0 | 1 | 2514 |
| 3.404 | 1.750 | 83.0 | 0.020 | 364.1 | 100 | 250 | 1 | 0.50 | 0 | 1 | 4054 |
| 2.086 | 1.751 | 50.0 | 0.020 | 362.8 | 200 | 250 | 1 | 0.50 | 0 | 1 | 1877 |
| 2.080 | 1.750 | 55.0 | 0.020 | 362.4 | 200 | 250 | 1 | 0.50 | 0 | 1 | 1971 |
| 6.056 | 1.751 | 60.0 | 0.020 | 363.8 | 200 | 250 | 1 | 0.50 | 0 | 1 | 2034 |
| 3.406 | 1.748 | 65.0 | 0.020 | 363.5 | 200 | 251 | 1 | 0.50 | 0 | 1 | 2626 |
| 3.420 | 1.750 | 70.0 | 0.020 | 363.7 | 200 | 250 | 1 | 0.50 | 0 | 1 | 3107 |

Table A.1: Experimental 2SLGG loading parameters used in regression model training and validation, as well as *measured* muzzle velocity for reference.

| Projectile Package Mass (g) | Primary Powder Mass (g) | Secondary Powder Mass (g) | Burst Disc Score Depth (in) | Piston Mass (g) | Target Tank Pressure (Torr) | Pump Tube Pressure (psi) | Volume Reducers | Piston Tightness | H4831SC | IMR 4831 | Projectile Velocity (m/s) |
|-----------------------------|-------------------------|---------------------------|-----------------------------|-----------------|-----------------------------|--------------------------|-----------------|------------------|---------|----------|---------------------------|
| 3.403 | 1.748 | 75.0 | 0.020 | 363.6 | 200 | 250 | 1 | 0.50 | 0 | 1 | 3234 |
| 3.403 | 1.750 | 75.0 | 0.020 | 363.3 | 110 | 250 | 1 | 0.50 | 0 | 1 | 3496 |
| 3.407 | 1.750 | 70.0 | 0.020 | 363.2 | 200 | 250 | 1 | 0.50 | 0 | 1 | 3107 |
| 3.405 | 1.752 | 83.0 | 0.020 | 363.5 | 110 | 250 | 1 | 0.50 | 0 | 1 | 3807 |
| 6.045 | 1.756 | 65.3 | 0.020 | 363.1 | 300 | 250 | 1 | 0.50 | 0 | 1 | 2264 |
| 6.055 | 1.749 | 65.0 | 0.020 | 361.9 | 495 | 260 | 1 | 0.50 | 0 | 1 | 1823 |
| 3.395 | 1.749 | 130.0 | 0.020 | 363.1 | 80 | 220 | 1 | 0.50 | 0 | 1 | 5933 |
| 3.416 | 1.750 | 85.0 | 0.020 | 363.1 | 100 | 250 | 1 | 0.50 | 0 | 1 | 3897 |
| 2.814 | 1.750 | 65.0 | 0.020 | 362.7 | 300 | 260 | 1 | 0.50 | 0 | 1 | 2434 |
| 2.198 | 1.751 | 65.0 | 0.020 | 362.8 | 305 | 251 | 1 | 0.50 | 0 | 1 | 2670 |
| 3.409 | 1.751 | 65.0 | 0.020 | 362.7 | 299 | 249 | 1 | 0.50 | 0 | 1 | 2435 |
| 3.403 | 1.751 | 60.8 | 0.020 | 362.9 | 193 | 251 | 1 | 0.50 | 0 | 1 | 2397 |
| 3.401 | 1.768 | 60.0 | 0.020 | 363.1 | 215 | 255 | 1 | 0.50 | 0 | 1 | 1966 |
| 6.010 | 1.746 | 70.0 | 0.020 | 364.6 | 196 | 256 | 1 | 0.50 | 0 | 1 | 2612 |
| 3.400 | 1.755 | 85.0 | 0.020 | 363.4 | 100 | 250 | 1 | 0.50 | 0 | 1 | 3580 |
| 3.384 | 1.749 | 60.8 | 0.020 | 363.0 | 215 | 253 | 1 | 0.50 | 0 | 1 | 2496 |
| 3.404 | 1.773 | 109.9 | 0.020 | 363.3 | 100 | 200 | 1 | 0.50 | 0 | 1 | 5307 |
| 3.366 | 1.750 | 90.0 | 0.020 | 363.2 | 100 | 220 | 1 | 0.50 | 0 | 1 | 3917 |
| 3.352 | 1.751 | 90.0 | 0.020 | 363.6 | 100 | 220 | 1 | 0.50 | 0 | 1 | 4409 |
| 3.391 | 1.751 | 80.0 | 0.020 | 363.4 | 100 | 220 | 1 | 0.50 | 0 | 1 | 3583 |
| 6.005 | 1.752 | 60.0 | 0.020 | 362.9 | 205 | 250 | 1 | 0.50 | 0 | 1 | 1816 |
| 6.013 | 1.752 | 60.0 | 0.020 | 363.1 | 197 | 250 | 1 | 0.50 | 0 | 1 | 1972 |
| 6.002 | 1.756 | 65.0 | 0.020 | 363.2 | 200 | 250 | 2 | 0.50 | 0 | 1 | 2629 |
| 6.048 | 1.751 | 65.0 | 0.020 | 363.4 | 199 | 250 | 2 | 0.50 | 0 | 1 | 2624 |
| 2.148 | 1.750 | 125.0 | 0.014 | 363.5 | 85 | 220 | 1 | 0.50 | 0 | 1 | 6369 |
| 2.122 | 1.752 | 125.0 | 0.014 | 363.6 | 85 | 272 | 1 | 0.50 | 0 | 1 | 5715 |
| 2.035 | 1.751 | 125.0 | 0.014 | 363.3 | 85 | 242 | 1 | 0.50 | 0 | 1 | 6018 |
| 2.139 | 1.751 | 125.0 | 0.014 | 363.5 | 85 | 242 | 1 | 0.50 | 0 | 1 | 6192 |

Table A.1: Experimental 2SLGG loading parameters used in regression model training and validation, as well as *measured* muzzle velocity for reference.

| Projectile Package Mass (g) | Primary Powder Mass (g) | Secondary Powder Mass (g) | Burst Disc Score Depth (in) | Piston Mass (g) | Target Tank Pres- sure (Torr) | Pump Tube Pres- sure (psi) | Volume Re- ducers | Piston Tightness | H4831SC | IMR 4831 | Projectile Velocity (m/s) |
|-----------------------------------|-------------------------------|---------------------------------|-----------------------------------|--------------------|-------------------------------------|----------------------------------|----------------------|---------------------|---------|----------|---------------------------------|
| 2.062 | 1.749 | 55.0 | 0.020 | 363.2 | 200 | 250 | 2 | 0.50 | 0 | 1 | 2493 |
| 6.065 | 1.750 | 60.0 | 0.020 | 363.5 | 199 | 251 | 2 | 0.50 | 0 | 1 | 2418 |
| 2.057 | 2.000 | 125.0 | 0.014 | 366.0 | 85 | 242 | 1 | 0.25 | 0 | 1 | 6274 |
| 6.041 | 1.753 | 75.0 | 0.020 | 366.3 | 102 | 250 | 2 | 0.75 | 0 | 1 | 3106 |
| 6.045 | 1.750 | 73.0 | 0.020 | 366.0 | 100 | 251 | 2 | 0.00 | 0 | 1 | 3087 |
| 2.138 | 2.001 | 125.0 | 0.014 | 366.1 | 90 | 250 | 1 | 0.00 | 0 | 1 | 5527 |
| 2.141 | 2.001 | 125.0 | 0.014 | 366.3 | 90 | 250 | 1 | 0.50 | 0 | 1 | 6070 |
| 2.095 | 1.749 | 55.0 | 0.020 | 366.1 | 149 | 249 | 2 | 0.00 | 0 | 1 | 2618 |
| 2.090 | 1.750 | 55.0 | 0.020 | 366.2 | 150 | 250 | 2 | 0.00 | 0 | 1 | 2372 |
| 2.052 | 2.002 | 125.0 | 0.014 | 365.9 | 92 | 250 | 1 | 0.25 | 0 | 1 | 6140 |
| 2.500 | 2.001 | 115.0 | 0.014 | 366.2 | 0 | 220 | 1 | 0.00 | 0 | 1 | 5856 |
| 2.043 | 1.999 | 110.0 | 0.014 | 365.8 | 90 | 250 | 1 | 0.50 | 0 | 1 | 5172 |
| 6.013 | 1.753 | 55.0 | 0.020 | 365.4 | 199 | 249 | 2 | 0.00 | 0 | 1 | 2116 |
| 6.022 | 1.749 | 73.0 | 0.020 | 366.3 | 200 | 250 | 2 | 0.00 | 0 | 1 | 2897 |
| 6.012 | 1.749 | 67.0 | 0.020 | 366.1 | 200 | 250 | 2 | 0.25 | 0 | 1 | 2749 |
| 6.026 | 1.751 | 67.0 | 0.020 | 356.9 | 199 | 249 | 2 | 0.50 | 0 | 1 | 2631 |
| 2.052 | 1.999 | 110.0 | 0.014 | 365.7 | 92 | 249 | 1 | 0.75 | 0 | 1 | 5453 |
| 6.058 | 1.752 | 73.0 | 0.020 | 365.9 | 198 | 251 | 2 | 0.50 | 0 | 1 | 2858 |
| 6.018 | 1.748 | 60.0 | 0.020 | 366.2 | 195 | 249 | 2 | 0.50 | 0 | 1 | 2520 |
| 6.014 | 1.750 | 57.0 | 0.020 | 366.0 | 196 | 250 | 2 | 0.25 | 0 | 1 | 2358 |
| 3.396 | 1.750 | 64.0 | 0.020 | 366.0 | 99 | 180 | 2 | 0.75 | 0 | 1 | 3207 |
| 3.376 | 1.751 | 75.0 | 0.020 | 366.2 | 99 | 251 | 2 | 1.00 | 0 | 1 | 3791 |
| 3.414 | 1.753 | 86.0 | 0.020 | 366.2 | 98 | 250 | 2 | 0.50 | 0 | 1 | 4244 |
| 3.367 | 1.750 | 100.0 | 0.020 | 366.1 | 85 | 250 | 2 | 0.50 | 0 | 1 | 4839 |
| 3.381 | 1.999 | 150.0 | 0.020 | 366.0 | 80 | 250 | 1 | 0.25 | 0 | 1 | 6542 |
| 2.007 | 1.750 | 55.0 | 0.020 | 366.0 | 149 | 250 | 2 | 0.25 | 0 | 1 | 2553 |
| 2.018 | 1.750 | 55.0 | 0.020 | 366.1 | 146 | 249 | 2 | 0.25 | 0 | 1 | 2486 |
| 3.367 | 2.002 | 125.0 | 0.020 | 366.2 | 80 | 230 | 1 | 0.25 | 0 | 1 | 5603 |

Table A.1: Experimental 2SLGG loading parameters used in regression model training and validation, as well as *measured* muzzle velocity for reference.

| Projectile Package Mass (g) | Primary Powder Mass (g) | Secondary Powder Mass (g) | Burst Disc Score Depth (in) | Piston Mass (g) | Target Tank Pres- sure (Torr) | Pump Tube Pres- sure (psi) | Volume Re- ducers | Piston Tightness | H4831SC | IMR 4831 | Projectile Velocity (m/s) |
|-----------------------------------|-------------------------------|---------------------------------|-----------------------------------|--------------------|-------------------------------------|----------------------------------|----------------------|---------------------|---------|----------|---------------------------------|
| 3.368 | 2.000 | 135.0 | 0.020 | 365.8 | 75 | 230 | 1 | 0.00 | 0 | 1 | 6144 |
| 3.371 | 2.001 | 130.0 | 0.020 | 366.1 | 80 | 231 | 1 | 0.00 | 0 | 1 | 5997 |
| 1.995 | 1.749 | 68.0 | 0.020 | 365.8 | 150 | 250 | 2 | 0.50 | 0 | 1 | 3057 |
| 2.001 | 1.750 | 68.0 | 0.020 | 365.9 | 147 | 249 | 2 | 0.75 | 0 | 1 | 3083 |
| 3.370 | 2.000 | 130.0 | 0.020 | 365.5 | 80 | 230 | 1 | 0.00 | 0 | 1 | 5924 |
| 2.056 | 2.002 | 110.0 | 0.014 | 366.4 | 90 | 250 | 1 | 0.75 | 1 | 0 | 5155 |
| 2.047 | 2.001 | 130.0 | 0.014 | 366.2 | 80 | 250 | 1 | 0.75 | 1 | 0 | 6317 |
| 2.060 | 2.002 | 125.0 | 0.014 | 366.1 | 80 | 250 | 1 | 0.50 | 1 | 0 | 5996 |
| 2.058 | 2.000 | 125.0 | 0.014 | 366.0 | 80 | 250 | 1 | 1.00 | 1 | 0 | 6351 |
| 2.074 | 1.755 | 68.0 | 0.014 | 366.1 | 100 | 250 | 2 | 1.00 | 0 | 1 | 3646 |
| 2.008 | 1.750 | 94.0 | 0.020 | 366.1 | 125 | 250 | 2 | 0.75 | 0 | 1 | 4768 |
| 2.001 | 2.021 | 130.0 | 0.014 | 366.1 | 100 | 250 | 1 | 1.00 | 1 | 0 | 6313 |
| 1.999 | 1.751 | 85.0 | 0.020 | 366.0 | 125 | 250 | 2 | 0.50 | 1 | 0 | 3628 |
| 3.380 | 2.001 | 127.0 | 0.020 | 365.6 | 80 | 230 | 1 | 0.00 | 0 | 1 | 5928 |
| 3.412 | 1.998 | 125.0 | 0.020 | 365.4 | 80 | 230 | 1 | 0.00 | 0 | 1 | 5747 |
| 3.376 | 2.003 | 150.0 | 0.020 | 366.0 | 80 | 250 | 1 | 0.50 | 1 | 0 | 6286 |
| 3.369 | 2.003 | 157.0 | 0.020 | 367.1 | 80 | 250 | 1 | 1.00 | 1 | 0 | 6355 |
| 2.003 | 1.750 | 88.0 | 0.020 | 366.5 | 125 | 250 | 2 | 0.75 | 1 | 0 | 3863 |
| 1.990 | 1.751 | 89.0 | 0.020 | 366.6 | 125 | 250 | 2 | 1.00 | 1 | 0 | 4232 |
| 2.005 | 1.751 | 88.5 | 0.020 | 366.8 | 125 | 250 | 2 | 1.00 | 1 | 0 | 4306 |
| 3.395 | 1.751 | 65.0 | 0.020 | 367.4 | 99 | 180 | 2 | 1.00 | 0 | 1 | 3449 |
| 3.370 | 2.004 | 110.0 | 0.020 | 365.8 | 85 | 240 | 1 | 1.00 | 1 | 0 | 5063 |
| 3.370 | 2.000 | 160.0 | 0.020 | 365.8 | 80 | 250 | 1 | 1.00 | 1 | 0 | 6791 |
| 3.415 | 1.006 | 160.0 | 0.020 | 366.8 | 80 | 250 | 1 | 1.00 | 1 | 0 | 6700 |
| 2.000 | 1.755 | 88.0 | 0.020 | 365.7 | 125 | 250 | 2 | 0.00 | 1 | 0 | 3819 |
| 2.013 | 1.751 | 88.0 | 0.020 | 366.0 | 125 | 250 | 2 | 0.50 | 1 | 0 | 4289 |
| 2.012 | 1.751 | 88.5 | 0.020 | 366.5 | 125 | 250 | 2 | 0.50 | 1 | 0 | 3867 |
| 1.968 | 1.751 | 88.0 | 0.020 | 366.5 | 125 | 250 | 2 | 1.00 | 1 | 0 | 4471 |

Table A.1: Experimental 2SLGG loading parameters used in regression model training and validation, as well as *measured* muzzle velocity for reference.

| Projectile Package Mass (g) | Primary Powder Mass (g) | Secondary Powder Mass (g) | Burst Disc Score Depth (in) | Piston Mass (g) | Target Tank Pres- sure (Torr) | Pump Tube Pres- sure (psi) | Volume Re- ducers | Piston Tightness | H4831SC | IMR 4831 | Projectile Velocity (m/s) |
|-----------------------------------|-------------------------------|---------------------------------|-----------------------------------|--------------------|-------------------------------------|----------------------------------|----------------------|---------------------|---------|----------|---------------------------------|
| 2.035 | 1.750 | 65.0 | 0.020 | 366.6 | 125 | 250 | 2 | 1.00 | 1 | 0 | 3197 |
| 2.039 | 1.755 | 65.0 | 0.020 | 363.5 | 126 | 251 | 2 | 1.00 | 1 | 0 | 2982 |
| 2.029 | 1.754 | 65.0 | 0.020 | 366.7 | 125 | 250 | 2 | 1.00 | 1 | 0 | 3086 |
| 2.029 | 1.756 | 65.0 | 0.020 | 365.7 | 125 | 250 | 2 | 1.00 | 1 | 0 | 3141 |
| 2.031 | 1.756 | 65.0 | 0.020 | 366.9 | 125 | 250 | 2 | 1.00 | 1 | 0 | 3131 |
| 2.029 | 1.752 | 65.0 | 0.020 | 365.1 | 125 | 250 | 2 | 1.00 | 1 | 0 | 3028 |
| 2.037 | 1.751 | 65.0 | 0.020 | 366.8 | 125 | 250 | 2 | 1.00 | 1 | 0 | 2964 |
| 2.042 | 1.748 | 65.0 | 0.020 | 366.5 | 125 | 250 | 2 | 1.00 | 1 | 0 | 3107 |
| 2.045 | 1.752 | 65.0 | 0.020 | 366.0 | 125 | 250 | 2 | 1.00 | 1 | 0 | 3167 |
| 2.026 | 1.750 | 65.0 | 0.020 | 366.0 | 125 | 250 | 2 | 1.00 | 1 | 0 | 3050 |
| 1.981 | 1.750 | 88.0 | 0.020 | 367.7 | 125 | 250 | 2 | 0.50 | 1 | 0 | 4625 |
| 1.991 | 1.751 | 88.0 | 0.020 | 367.0 | 125 | 250 | 2 | 0.50 | 1 | 0 | 4312 |
| 2.034 | 1.751 | 65.0 | 0.020 | 366.8 | 125 | 250 | 2 | 1.00 | 1 | 0 | 3186 |
| 1.982 | 1.751 | 65.0 | 0.020 | 366.0 | 125 | 250 | 2 | 1.00 | 1 | 0 | 3067 |
| 2.043 | 1.749 | 65.0 | 0.020 | 366.7 | 125 | 250 | 2 | 1.00 | 1 | 0 | 3106 |
| 1.974 | 1.749 | 88.1 | 0.020 | 366.2 | 125 | 250 | 2 | 0.50 | 1 | 0 | 3659 |
| 1.982 | 1.750 | 130.0 | 0.014 | 366.0 | 125 | 250 | 1 | 0.00 | 1 | 0 | 6219 |
| 6.063 | 1.749 | 55.0 | 0.020 | 362.9 | 250 | 250 | 2 | 0.00 | 1 | 0 | 1785 |
| 1.979 | 1.751 | 100.0 | 0.014 | 366.0 | 115 | 250 | 1 | 0.00 | 1 | 0 | 4088 |
| 2.085 | 1.750 | 115.0 | 0.014 | 362.9 | 95 | 250 | 1 | 0.00 | 1 | 0 | 4706 |
| 1.988 | 1.750 | 75.0 | 0.014 | 363.1 | 110 | 250 | 2 | 0.00 | 1 | 0 | 3123 |
| 1.988 | 1.751 | 72.0 | 0.020 | 363.1 | 100 | 250 | 2 | 0.00 | 1 | 0 | 2835 |
| 1.971 | 1.749 | 120.0 | 0.014 | 363.1 | 89 | 250 | 1 | 0.00 | 1 | 0 | 4902 |
| 6.059 | 1.751 | 55.0 | 0.020 | 363.1 | 275 | 250 | 2 | 0.00 | 1 | 0 | 1558 |
| 6.026 | 1.751 | 56.0 | 0.020 | 363.1 | 225 | 250 | 2 | 0.00 | 1 | 0 | 1996 |
| 1.986 | 1.750 | 73.0 | 0.020 | 362.8 | 100 | 250 | 2 | 0.00 | 1 | 0 | 2997 |
| 1.986 | 1.754 | 128.0 | 0.014 | 362.9 | 83 | 250 | 1 | 0.00 | 1 | 0 | 5485 |
| 1.979 | 1.748 | 121.0 | 0.014 | 362.9 | 90 | 250 | 1 | 0.00 | 1 | 0 | 4866 |

Table A.1: Experimental 2SLGG loading parameters used in regression model training and validation, as well as *measured* muzzle velocity for reference.

| Projectile Package Mass (g) | Primary Powder Mass (g) | Secondary Powder Mass (g) | Burst Disc Score Depth (in) | Piston Mass (g) | Target Tank Pres- sure (Torr) | Pump Tube Pres- sure (psi) | Volume Re- ducers | Piston Tightness | H4831SC | IMR 4831 | Projectile Velocity (m/s) |
|-----------------------------------|-------------------------------|---------------------------------|-----------------------------------|--------------------|-------------------------------------|----------------------------------|----------------------|---------------------|---------|----------|---------------------------------|
| 1.979 | 1.750 | 100.0 | 0.014 | 362.9 | 115 | 250 | 2 | 0.00 | 1 | 0 | 4649 |
| 1.979 | 2.002 | 100.0 | 0.014 | 363.0 | 114 | 250 | 2 | 0.00 | 1 | 0 | 4663 |
| 1.972 | 1.752 | 121.0 | 0.014 | 363.2 | 95 | 250 | 1 | 0.00 | 1 | 0 | 5899 |
| 5.979 | 1.750 | 65.0 | 0.020 | 362.6 | 195 | 251 | 2 | 0.00 | 1 | 0 | 1987 |
| 5.925 | 1.752 | 67.0 | 0.020 | 363.4 | 195 | 250 | 2 | 1.00 | 1 | 0 | 2687 |
| 6.030 | 1.750 | 75.0 | 0.020 | 370.3 | 105 | 249 | 2 | 0.50 | 1 | 0 | 2619 |